Lifetesting GaAs MMICs Under RF Stimulus

William J. Roesch, Tony Rubalcava, and Clark Hanson

Abstract—**This paper summarizes very high temperature lifetest results on MMIC switches and attenuators designed, assembled and screened by Motorola GEG and manufactured and tested by TriQuint. It was found that individual heating and RF bias resulted in data which indicates the devices degrade linearly with lognormal failure distributions that compare favorably with historical dc lifetesting of MMIC amplifiers. Electrical measurements indicated MESFET gate degradation was occurring, which was confirmed by failure analysis. The failure mechanism was found to be highly accelerated by temperature and is not expected to impede device lifetimes at normal use conditions for thousands of years.**

Introduction

As GALLIUM arsenide Monolithic Microwave Integrated Circuits (MMICs) mature, focus shifts from performance and manufacturability issues to factors that influence suitability in widespread military and commercial applications, like device reliability. Concerns about reliability therefore signal the move of emerging technologies from being laboratory curiosities to being inserted into systems.

There is little historical data on non-amplifier MMIC reliability. This study addresses MMIC switch and attenuator lifetesting performed under RF bias and high temperature conditions. In addition to the rare look into small signal device reliability, this investigation incorporated a test system which precisely controlled temperature at the case of each device. Use of this system resulted in thermal consistency never before achieved in such a lifetest. Individual heating of the device case also allowed high frequency fixturing to be employed, which under usual circumstances would be significantly degraded by conventional oven or hotplate techniques. This new approach facilitated premium *S*-parameter measurements throughout the 4380-hour lifetest. The combination of precise temperature control and high quality device measurement resulted in accurate prediction of device reliability with relatively few devices.

Test Vehicles

MMICs for this study were designed by Motorola GEG and manufactured using TriQuint's ion implanted 0.5 μm depletion mode GaAs MESFET process. Recessed gates were composed of titanium/palladium/gold, as was the first layer interconnect metallization. Airbridge metal was fabricated from electroplated gold on a titanium flash. Thin film resistors were made from Nichrome, and capacitors and dielectrics were PECVD nitride.

Two types of structures have been utilized in this investigation, single-pole, single-throw (SPST) switches and voltage-controlled attenuators (VCAs). The SPST switch contains two series MESFETs with three shunt MESFETs to achieve a minimum 55 dB ON/OFF amplitude ratio and 1.8 dB maximum insertion loss. The VCA contains two series MESFETs and two shunt MESFETs, where the gate voltages control the overall attenuation. A 40 dB minimum attenuation and 28 dB of linear tuning range is required per specification.

All circuits used in this study were assembled by Motorola GEG in a metal-based, glass side-walled package, using a gold/tin eutectic die attach process, 1 mil automatic gold ball bonding, and gold/tin lid sealing. All devices were subjected to Motorola GEG's standard Class S screening which consists of internal visual inspection, temperature cycling, constant acceleration, particle impact noise detection (PIND), initial electrical testing, 240 hour burn-in at 125°C ambient, final electrical, and hermeticity tests. No samples were rejected from the production lot for failing burn-in delta requirements, as has been the case with all Motorola-TriQuint product to date.

Fixtures

The fixtures which house the test devices must fulfill four requirements: 1) withstand the high temperatures of accelerated reliability testing, 2) allow electrical measurements at rated frequencies, 3) provide RF stimulus and 4) allow dc monitoring by lifetest system. Because of the unique approach of heating each device individually at the case, the requirements of high temperature fixturing was significantly reduced. An Engineering Test Fixture (ETF) was used (Fig. 1). Since heat applied to the case (in excess of 260°C) was conducted out the device leads to some extent, high temperature solder was used to attach the test devices and a polyimide circuit board was utilized instead of teflon or duroid. A stripline approach was used on the polyimide, and two iterations of design and fabrication were needed to achieve a good 50 Ω match. All high temperature interface problems were addressed by device attachment and circuit board composition, so conventional high frequency fixturing could be used in the remainder of the fixturing. For example, SMA connectors and semi-rigid coaxial cable utilizing teflon dielectric

Manuscript received March 31, 1992; revised July 28, 1992.

W. J. Roesch and T. Rubalcava are with TriQuint Semiconductor, P.O. Box 4935, Beaverton, OR 97076.

IEEE Log Number 9203963.

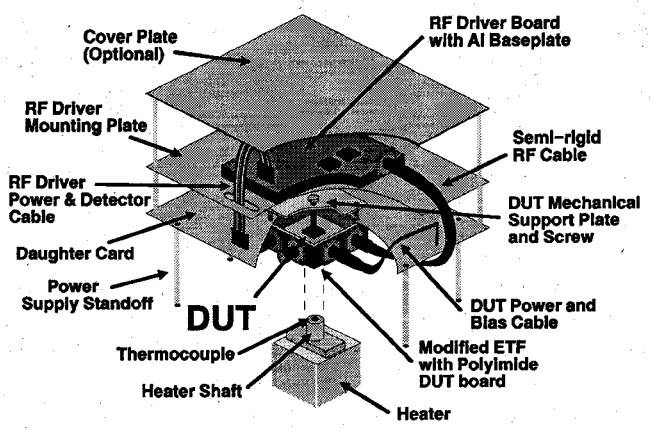

Fig. 1. Diagram of the engineering test fixture mounted in the fixture assembly.

could be employed without fear of melting. RF stimulus was generated within inches of each part by individual GaAs voltage-controlled oscillators. For the switch, additional broad band amplification was accomplished with a distributed amplifier MMIC. Drive signal levels were nominally 0.7 and 0.6 GHz at +13 dBm and 0 dBm for the switch and attenuator, respectively. This stimulus was selected to exceed the worst case levels expected in normal use by 1 dBm. The lifetest system monitored power supply voltages and currents to each device under test, as well as voltage from a detector used to measure RF power delivered through each test device.

Temperatures and Thermal Resistance Measurements

The samples of switches were subjected to peak hotspot temperatures of 235° and 260°C and the attenuators were subjected to peak hotspot temperatures of 225° and 250°C. The temperatures were staggered for two reasons. First, if the devices failed for similar mechanisms they could be grouped for analysis. Secondly, a wider range of temperatures would give the best chance for failures to occur during the test. The temperatures were selected based on previous circuit testing and thermal analysis results. The low end of the temperature window was selected to force the widest failure distributions in time. Therefore, the highest risk was that few or no failures will occur within the six month time under test.

Determining device temperatures is a key part of any reliability study, especially if activation energies are to be determined accurately. There are several possible methods for measuring temperature, but each has advantages and significant problems. Temperatures of the entire IC package environment were evaluated from case to hotspot. For data analysis, the temperature of the failure site must be known.

Complete thermal analysis includes both infrared thermal imaging and liquid crystal microscopy. The data from infrared analysis, which shows how average temperatures on the die vary with case temperature and/or biasing conditions, can be combined with the liquid crystal result, which shows the precise hotspot absolute temperature, and used to predict die hotspot temperatures for a wide range of applications. Thermal measurements were made with sample devices and special test chips to guarantee that the device hotspot (MESFET channel, for this study) temperatures were within 5°C of the specified absolute temperatures while being individually controlled within 0.5°C of the setpoint during the entire test.

Step Stress Test

Determination of the lifetest temperatures for this program was one of the key problems. Generally, step stress tests are performed to help determine the best lifetest temperatures. Additionally, step stress tests are performed to 1) determine if the electrical measurements are repeatable, 2) prove-out the test fixturing, 3) check devices for anomalous high temperature operation, and 4) to get a preliminary look at the types of failure mechanisms to expect during subsequent lifetesting. Originally, step stress testing was intentionally omitted from this program. Once the program was started, it was determined that there was too much at risk to proceed into the lifetest without a step stress test, so an abbreviated test was conducted with the devices examined in the thermal analysis portion of the program.

There were two samples of attenuators, and two switch samples examined in the thermal analysis. The switches and attenuators were rinsed to remove as much of the liquid crystal as possible, and then the package lids were resoldered in place (not sealed). These four devices were then soldered into ETFs, measured initially, and started on a step stress test. The step stress test was started at 200°C, and the temperature was increased 25°C after each 24 hour interval. Both attenuators and switches withstood step stressing to 275°C without degradation or failure. The maximum long term capability of the lifetest system was known to be 260°C. Continued testing at 275°C would result in premature wearout of the heaters, so the step stress devices were continued at 260°C using 48 hour measurement intervals.

Based upon the original ramp data, it was determined that the highest possible temperatures should be utilized for the lifetest. The network analyzer measurements were found to be very stable and repeatable over time. The devices had no quirky problems at high temperature. They behaved normally without anomalous increases in power consumption. As in the subsequent lifetesting, there was not enough degradation to predict what type of failure mechanisms might occur with these devices. The step stress testing accumulated 960 hours on attenuators and 1008 hours for switches at 260°C.

The big advantage of the step stress testing came when two anomalous mechanical failures were inadvertently created. Part #269, a switch, failed because of a die crack after the initial ramp to 275°C and 240 additional hours at 260°C. Part #199, an attenuator, failed because of extreme mechanical stress when its polyimide stress relief

pad fell out after the initial ramp to 275°C and 288 hours at 260°C. In addition to discovering the potential for high mechanical stress in the fixtures, the occurrence of stress relief screws actually "backing-out" of their threads during testing was uncovered. Because of this information, extra precautions were taken early with the lifetest fixturing. The stress relief screws were epoxied in place and the polyimide pads which were placed between the stress relief screws and package bodies, were also epoxied to the screws. In addition to these mechanical changes, more care was used in handling the devices because of their susceptibility to mechanical damage. After experiencing additional difficulties in the lifetesting, we also added spacers to the fixturing so that the heater spring force was minimized. Thus, by running just four devices, we are able to set the optimum lifetest temperatures and take precautions which limited the anomalous fallout of devices. This was a critical phase of the program that contributed to its success.

Accelerated Life Test Overview

A total of four 4380 hour accelerated lifetests were conducted, two on switches and two on attenuators. The lifetests were conducted at 225° and 250°C for attenuators and 235° and 260°C for switches. Interim measurements were made at 4, 8, 16, 32, 64, 128, 256, 512, 1024, 1536, 2048, 2624, 3200, and 3790 hours. Five device samples were used at each temperature. Two measurement control devices were used for the switch and two were used for the attenuator.

Data Collection

The devices were electrically characterized using an HP8510 Network Analyzer. The endpoint measurements made with the network analyzer were extremely successful. In addition to the two specific parameters used as failure criteria, 14 other parameters were monitored throughout the lifetesting. Data was collected for each of the 16 electrically measured parameters at each of the 16 test points, for each of the twenty test devices and two control devices, for a total of more than 5600 data points. The key parameters, ones used to determine failure, were S_{21}-ON AVE and S_{21}-OFF AVE. S_{21}-ON AVE is basically the insertion loss (expressed as gain) of either a switch or attenuator. It is measured with the respective device biased on its "ON" mode. S_{21} is then recorded at each 50 MHz interval from 0.35 GHz to 1.2 GHz for the switch and from 0.45 GHz to 0.86 GHz for the attenuator. These 18 or 8 S_{21} numbers are then averaged for the switch and attenuator, respectively. The S_{21}-OFF measurement is made the same way, except the "ON" pin for switches is grounded and the two control voltages on the attenuators are reversed. These were the two measurements to be used to assess device performance whereas a 1 dB change in the ON mode or a 5 dB change in the OFF mode would be considered a failure. The other parameters were also measured throughout the testing for informational reasons. The results were examined statistically (in terms of average numbers and standard deviations) and graphically.

Statistical indicators showed that device measurements were extremely stable over the one year span of the electrical measurements. Although only two of the twenty parts tested degraded enough to be classified as failures, the statistical data provides some interesting information. The results are particularly useful in assessing the stability of the measurement system and in examining how the S parameters degrade. For example, the standard deviations for the attenuator control devices were less than 0.05 dB for all of the S parameters throughout the entire test. And for the key parameters, the standard deviations were less than 0.02 dB! Even though the control devices exhibited some slight degradation during the testing (one control switch actually failed anomalously), the standard deviations of the parameter changes are good indicators of the variance in the measurements and the stability of the test set over time. The data can also be used to get more insight into how the devices were degrading. Using the 260°C switch data (the highest stressed condition exhibiting the most degradation) as an example, the biggest absolute changes, average changes, and largest standard deviations in insertion loss occurred at the low (0.35 GHz) end versus the high (1.2 GHz) end of the device's specified frequency range of operation. This observation is also true for isolation, but the numbers are not as conclusive as in the "ON" mode. Most of the frequency locations of maximums and minimums of the insertion loss or isolation, remained stable in terms of frequency. In other words, the S-parameter peaks and troughs characteristic of each device remained generally stable throughout the lifetesting, even when degradation occurred.

The second form of summarizing the measurement data is by graphical trend charts. These charts were developed to convey interim results for periodic reporting throughout this program. In all, 16 graphical charts were accumulated, covering each of the four test conditions in the ON and OFF modes for actual data and for changes from the initial measured parameters. Three examples of the graphical charts are shown in Figs. 2, 3, and 4. It is felt that the delta charts are superior for assessing the data since each device is depicted in relative terms. For example, some of the measurement capability variation is visible in the 225°C and 235°C lifetest results. The 235°C insertion loss is shown in Fig. 2. The variation is clear where all the devices take a dip at 2048 hours, and then recover at 2624 hours. These minor (about 0.02–0.04 dB) shifts and corrections are not obvious in the higher temperature results where the actual device degradation is more significant. In addition to the minor measurement glitches, several other results of the tests are clear from the delta charts. For example, the anomalous die cracking failure of part #17 in the 250°C attenuator test (and also part #340 in the 260°C switch lifetest) is obvious. The anomalous nature of this particular mechanical failure was clear in the isolation chart, shown in Fig. 3, not neces-

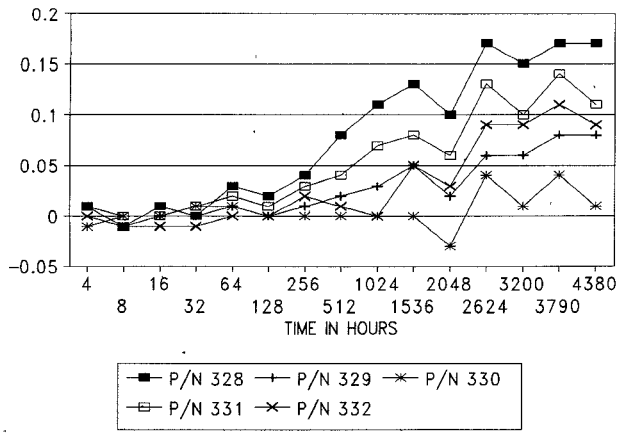

Fig. 2. 235°C lifetest on switches. Change in dB for S21-ON (AVG).

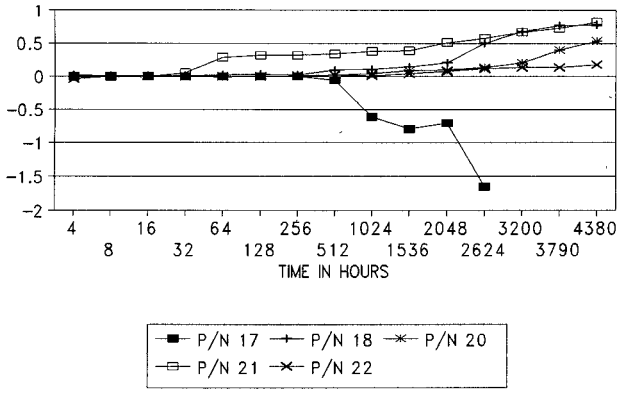

Fig. 3. 250°C lifetest on attenuators. Change in dB for S21-OFF (AVG).

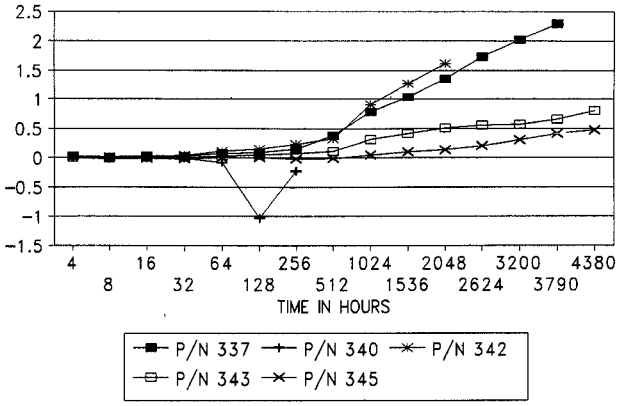

Fig. 4. 260°C lifetest on switches. Change in dB for S21-ON (AVG).

sarily because the degradation was significant, but because it was in the opposite direction from the other devices. The actual "failures" of parts #342 and #337 in the 260°C switch test between the 1024 and 1536 hour test points is also clear from 260°C switch lifetest delta chart in Fig. 4.

Failure Analysis

Failure analysis is necessary to identify each failure mechanism and classify each device for data analysis. A failure analysis procedure was developed before testing began. The procedure involved many interrelated steps depending on failure modes and the relative performance of the main population of devices. Precautions were taken to confirm device degradation, and ensure a positive identification of each failure. In the worst case scenario, mechanical circuit surgery would be required to identify what parts of the device have caused the failure. Due to the low complexity of the devices in this lifetest, mechanical surgery was expected to be conclusive in locating the failure if all other methods failed.

As per standard TriQuint procedure, each failed device was not removed as a failure until it exceeded the failure criteria twice during the standard interim measurements during the testing. If the failures were demonstrating anomalous electrical behavior, failure analysis was started without additional testing. For the slowly degrading devices, it was decided that continuation of the testing beyond the official failure criterion would help to exacerbate the physical failure to make it easier to determine the failure mechanism. Under this premise, part #337 was lifetested for the entire 4380 hours, even though it officially "failed" at the 1536 hour test point.

The first step of the failure analysis process required that the ETF be removed from the lifetest system fixturing. Once removed, a visual inspection could then be made. All solder joints on the package leads and SMA connectors were examined. If bad connections were discovered, they were documented and repaired. If repeated electrical measurements determined the device was good, then testing was continued. After the visual connection check, electrical measurements were made. These measurements were made three ways. First, pin-to-pin resistance measurements were made using a hand-held resistance meter. Then pin-to-pin curve tracer measurements were made. Lastly, a Time Domain Reflectometer (TDR) was used. This combination of measurements was usually effective in determining if the die was cracked, or if there was an electrical discontinuity inside the package. There curve tracer measurements were also found to give very good insight in the device degradation.

Once all external measurements were made, the device was unsoldered from the ETF, and the lid was removed. This was a very delicate operation. With the lid removed, we performed internal visual inspection optically up to 1000×. If die cracking was being confirmed, the package would be re-soldered into the ETF for follow-up measurements. In all cases of die cracking, the electrical behavior after lid removal correlated to the original measurements. In some cases, the performance after lid removal was more significantly degraded, because of the additional mechanical flexing and degradation to the cracks in the package de-soldering and lid removal processes.

The electrical testing and internal visual inspections on the degraded switch "failures" did not pin point the cause of degradation. We noticed some discoloration of 1st layer metal near ohmic metal connections, but additional SEM

inspection revealed no conclusive evidence for the cause of "failure." To help isolate the degrading portion of the circuit, switch #377 was submitted for circuit surgery. Several airbridges were mechanically broken so that each MESFET was isolated. Point-to-point measurements were then made with probes and a curve tracer. There was an obvious degradation of the MESFET parameters in the failed device. Example results of curve tracer measurements are shown in Fig. 5.

In general, the electrical measurement data proved to be a key indicator in the failure analyses. Degradation that occurred with abrupt magnitude and/or which occurred in the opposite direction from the main population of devices was a clear indication of mechanically induced failure. The mechanical failures also demonstrated characteristic parametric changes that were measured as part of the failure analysis procedure. For example, high dc resistance or abrupt discontinuities in the Time Domain Reflectometry results, clearly indicated cracking.

Using the example shown in Fig. 5, the source of the MESFET degradation could be investigated. Assuming the degradation is caused by gate or ohmic degradation, pure ohmic influence was ruled-out since the pinch-off changed. Expected ohmic degradation would probably only account for an increase of a few ohms. Without conclusive electrical data, physical analysis was attempted. To analyze the MESFETs physically, focused ion beam cross-sectioning was conducted.

Focused Ion Beam (FIB) is a relatively new analytical technique. The FIB operates similarly to a scanning electron microscope (SEM). But instead of focusing electrons on the sample, gallium ions are used. Imaging is achieved by collecting secondary electrons and/or ions from the resulting "milling" that occurs when the gallium ions impinge at the sample surface. As in the SEM, sometimes the sample can charge in the FIB. We found the charging to be minimal in the FIB, but the samples were coated with carbon to improve the imaging which was performed later in the SEM. In some cases, the FIB imaging is better than with a SEM, but as the magnification is increased, the ion milling becomes acute and the sample can be consumed quite rapidly. The FIB has many applications, but for this analysis, it was used to cut several micro cross-sections into the MESFETs. Parts #346 and #337 were both cross-sectioned, so that a comparison could be made between virgin and degraded devices. In practice, the cross-sectioning is achieved by milling several rectangular shaped areas in the surface of the sample in a stair-step configuration. These steps into the die created a wedge shaped viewport.

Although FIB experience with GaAs is very limited, we found the milling to be very fast. A nine micron wide by two micron deep cross-section was cut in about 5 minutes. After the viewing wedge is cut, the cross-section is "polished" by additional milling along the face of the cut. The polish is achieved by using a lower energy ion beam with a smaller spot size, focused along a line at the edge of the cross-section face. The polish also removes debris thrown onto the cross-section face during the gross milling process.

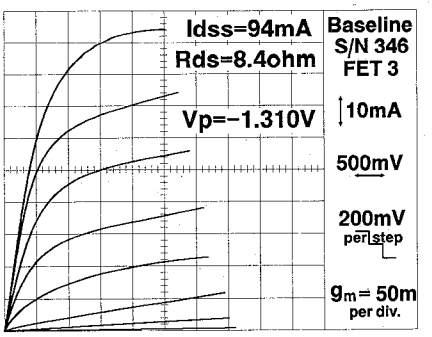

(a)

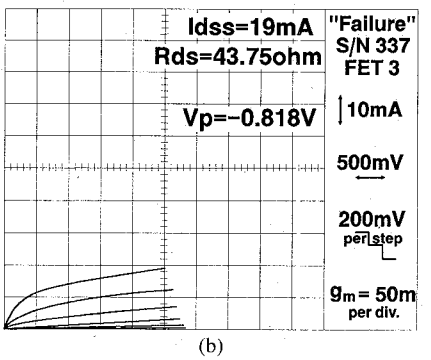

(b)

Fig. 5. Example curve tracer results. FET #3 is shown for both traces. Part #346, a reference switch, is shown on top, (a) and Part #337, a degraded switch, is shown below, (b).

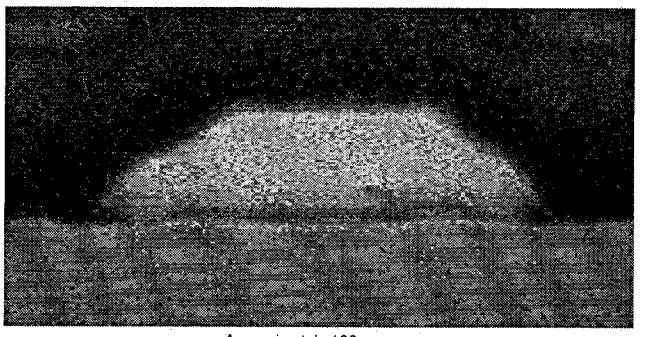

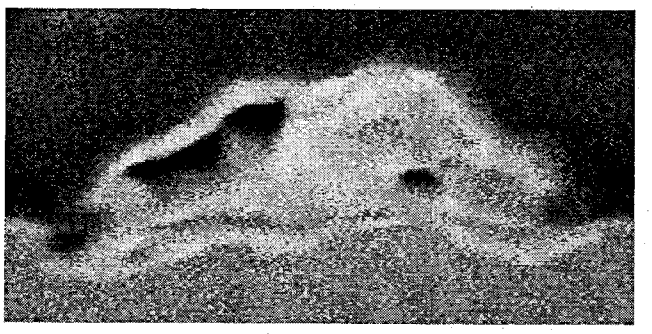

Fig. 6. SEM images of FIB cross-sections on a reference gate and a degraded gate. (45° tilt).

Imaging in the FIB was found to be inadequate for observing the features we were interested in, so the cross-section surfaces were given a final polish and not FIB im-

aged to maintain an undamaged face. In all, four cross-sections (2 polished) were made into FET #3 on the degraded device, and two cross-sections (1 polished) were made into FET #3 on the reference device. FIB cross-sectioning was performed by Milt Jaehnig of FEI Company, Beaverton, Oregon. After FIB, the samples were immediately taken to a TriQuint field emission SEM for imaging. SEM inspections of the cross-sections were made between 12 000× and 50 000×. The SEM image in Fig. 6 was made at 2 KVolts, 15 mm working distance, and at 45° angles to the die surface. The results were dramatic and conclusive. The gate metal has clearly diffused into the surface of the gallium arsenide on the degraded device, leaving voids. This diffusion is sometimes referred to as "sinking gates."

Analysis Methodology Overview

To obtain reliability statistics on MMICs, the cumulative failure distribution of the device samples must be measured. Generally, highly accelerated aging conditions are required to generate a failure distribution. For GaAs MMICs, high temperature lifetesting has been found to be an effective method to find failure distributions in a reasonable time frame. Because of the acceleration used, the failure distributions created by high temperature lifetesting must be translated to normal use conditions. This translation involves activation energy calculations which are the subject of the next section.

All of the devices were grouped into two populations. The minor population included the two test devices which failed for anomalous mechanical problems. These devices were excluded from the main population and no further calculations were made on these anomalies. The rest of the devices were analyzed by part type and eventually grouped into one population. Degradation was minimal for all devices, but sufficient to predict eventual time to failure for all tests with the possible exception of the 225°C attenuators in the "OFF" condition. Even assuming reduced failure criteria of 1 dB, 0.5 dB, or 0.25 dB, changes in isolation were inadequate in helping predict times to failure because the degradation was so minimal that it appeared to be random. In fact, two attenuators increased in isolation, two decreased, and one virtually stayed the same. Otherwise, time to failure for each device was predicted by fitting the degradation to a straight line and extrapolating times to various failure criteria. These predicted failure times for each lifetest population were found to fit to lognormal distributions. The lognormal distribution parameters, median life (t_m) and sigma (σ), were calculated using another least squares fit. Activation energies were calculated for each part type, degradation fit, and failure criteria. Activation energy curve fits were also calculated for both device types pooled together. Parameter calculations were performed on a personal computer.

Distribution Calculations

Semiconductor integrated circuits in general, and GaAs ICs in particular have been found to fail in lognormal distributions. Because of the small sample sizes tested in this study, it is impossible to conclusively "prove" a lognormal failure distribution, and highly unlikely that an alternate distribution could be indicated. Therefore, a lognormal distribution was assumed, and in spite of the small sample sizes, all the degradation observed in this study appears to indicate this assumption is correct.

Before the failure distributions can be determined, the failures must be created. In this study, only two devices, switches at 260°C, were caused to exceed the predetermined failure criteria of a 1 dB change in insertion loss or a 5 dB change in isolation. Unfortunately, both failures occurred in the same time interval, so in reality, there is only one data point to plot for all four lifetests. One data point can also be "bounded" for each lifetest (a second point for 260°C switches) by assuming that one failure occurs at the end of the lifetest. This would be a worst case assumption, and provide the most conservative limit for estimating failures.

All is not lost, however. Because of the ability to make precise electrical measurements throughout the lifetesting, the degradation occurring during the study could be analyzed, and predictions could be based upon trends that were discovered. The delta plots shown in Figs. 2–4 could be used to a ss the device degradation, but care must be used since the time intervals are not to scale. However, the degradation can be "eyeballed" by noting that the intervals beyond 512 hours (found at the middle of the plots), are in approximate 500 hour spaces. Thus, by observing the change that occurs from the mid-point of the graphs to the end of the test, one could get an idea of the type of degradation exhibited by the devices, even though the vertical scales are not all equivalent. In our opinion, the devices were degrading in a linear manner. To investigate this observation mathematically, the degradation to was fitted to several types of curves. The data was plotted linearly, logarithmically, and exponentially. From this data, it was obvious that the degradation is not logarithmic, but linear and exponential curve fits came out nearly equivalent. We calculated failure distribution parameters using both linear and exponential fits. In all four lifetests, the fitting parameters (coefficients of determination) were equal out to three digits. In some tests, the exponential fit was slightly better, but linear curves were selected for predictive calculations because they matched the test with the most degradation (260°C switches) better, and because the resulting activation energy plot for all four tests was slightly more linear.

In practice, the observed degradation was fit to a line, and the line was used to estimate when a device would fail. This technique not only allows for predictions of when devices may reach the failure criterion sometime in the future (beyond the limits of the data), but also allows for the interpolation of a precise time to failure when de-

vice degradation actually exceeds the failure criterion. Thus, a more accurate time to failure can be calculated than by using the time of the test interval when the failure is first detected. For each test, the degradation data was arranged in a matrix and the curve-fitting was performed as a vector operation on the matrix. Once the best-fit lines were generated for each device's degradation, their intercepts were determined with several failure criteria. In this manner, the times to failure for various failure criteria could be easily generated by changing the intercept calculations. Once the times to failure were determined, they were sorted so that the failure accumulation for each point could be assigned. For example, the first failure out of five would be 20% accumulation, the second failure would be 40%, and so on. In the tests, where anomalous cracked devices were removed, the accumulation was made in 25% intervals.

In addition to characterizing the degradation, an investigation was made into the effects of failure criteria on distribution and acceleration factor parameters. This investigation was performed by looking at failure criteria of 0.5 dB and 0.25 dB changes for switches and attenuators in the "ON" condition, and for 1 dB, 0.5 dB, and 0.25 dB criteria for the devices in the "OFF" condition. The original 5.0 dB change criterion for the devices "OFF" (isolation) was so large compared to the observed degradation, that it would not be an issue in the wearout of these devices.

In general, all fits of the linear degradation to the lognormal distribution were very good (see Fig. 7), with coefficients of determination above 0.9. When 5 samples survived the test, the fits to lognormal were better than for the results from the tests which had anomalous cracks reducing the sample size to four. The tests fitting worst to lognormal distributions were the 225°C attenuator tests in the OFF condition and all conditions for the 260°C switch test. We felt the 225°C attenuator tests based upon a 1 dB change in isolation had insufficient degradation to make predictions. This was apparent by the extremely high sigma of over 1.8 in the OFF condition and extremely low sigma of 0.194 in the ON condition. No other sigmas exceed 1.1 and the average for a 1 dB change criterion is 0.701. The linear prediction of median life for the 225°C attenuators in the OFF condition was also over 5.5 times higher that the ON state median life.

The relatively poor fit of the 260°C switch results to a lognormal distribution is believed to be primarily caused because of the reduced sample size. With only four samples, the degradation data for the ON condition appears to be bimodal. But degradation in the OFF state is more evenly distributed between the four samples. We feel this indicates that there is truly a single distribution, but the small sample size results in a "choppy" straight line for the "ON" condition.

Activation Energy Calculations

Once the lognormal failure distribution parameters were determined for at least two different test temperatures,

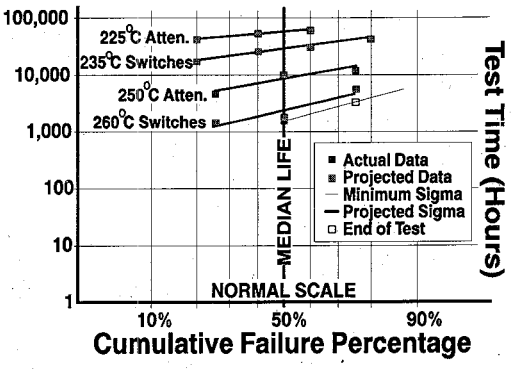

Fig. 7. Lognormal results based on projections of the data.

then an estimate of the accelerating effect of temperature could be made. For the switch and attenuator, the acceleration could be determined, but with only two points (data for two lifetests temperatures), a mathematical relationship between temperature and lifetimes could not be proven. Because of this limitation, it must be assumed that the switch and attenuator behave similarly to other GaAs devices and follow the Arrhenius relationship. The Arrhenius Reaction Rate equation for integrated circuits is:

$$\text{Acceleration Factor} = \exp -\frac{E_a}{K}\left(\frac{1}{T_2} - \frac{1}{T_1}\right)$$

where

E_a = activation energy in electron volts
K = Boltzmann's Constant = 8.61423 × 1e–5 eV/K
T = Absolute Temperature in Kelvin.

By common definition, the acceleration factor is the median life at low temperature divided by the median life at higher temperature. The median lives are determined by the methodology described in the previous section and the temperatures are the lifetest temperatures (converted to Kelvin). The remaining unknown value is the activation energy. With just two temperatures, the activation energy can be determined by direct substitution. For more temperatures, the activation energy can be determined by graphical plotting. As with lognormal plotting, activation energy plotting can be more precisely done mathematically. This was accomplished by converting the time scale to log, and inverting the temperature, then performing a least squares linear fit. Once the slope of the time/temperature relationship is known, it can be divided into Boltzmann's constant to determine the activation energy. The conversions can also be performed prior to graphing by converting each axis, then plotting. Fig. 8 shows an example of the result.

In this study, activation energies were calculated for several different conditions. Calculations were made using exponential degradation predictions of the failures with attenuators and switches operating in the "ON" condition and for linear degradation predictions of both devices in both "ON" and "OFF" states. For each of these six instances, activation energies were calculated for three

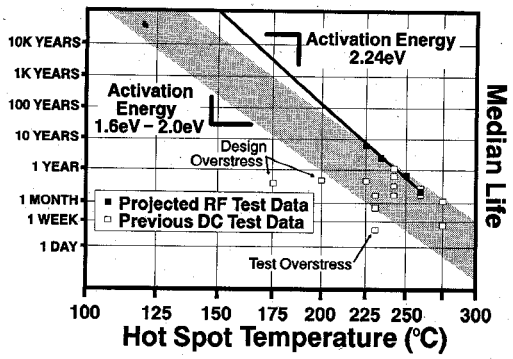

Fig. 8. Comparisons of results with other dc biased lifetests.

failure criteria: 1 dB, 0.5 dB, and 0.25 dB change. This resulted in eighteen activation energies which were each calculated from results measured at two temperatures. Additionally, we grouped results from attenuators and switches together, as if they were the same design, and predicted an additional nine activation energies based upon four data points. Because of the near zero degradation encountered with the attenuators in the "OFF" state, additional activation energies were calculated using just three points (250°C attenuators, 235°C switches, 260° switches). Omitting the 225°C attenuators resulted in activation energies much nearer to those obtained for all four devices in the "ON" state, and also near perfect straight line Arrhenius fits. Ignoring the anomalous data for 225°C attenuators in the OFF condition, the calculated activation energies ranged from 1.6 to 2.7 eV in this study. The most accurate activation energy is 2.24 eV, based on the degradation predictions of all four lifetests lumped together with a 1 dB failure criterion.

Once the activation energies are known, predictions can be made to estimate reliability at operational conditions. For these estimations, the most conservative activation energy, 1.6 eV, was selected and applied to the least reliable projected data point. This data point was for 260°C switches (which actually had the highest calculated activation energy). Using the Arrhenius equation and 1.6 eV activation energy, an equivalent median life for normal operation compared to lifetest conditions can be calculated. The acceleration factor from 260°C to 150°C for an activation energy of 1.6 eV is 8660.67. So an expected median lifetime would be the predicted median life (2148 hours) multiplied by the acceleration factor, or 18.7 million hours (which is 2138 years). Using the highest activation energy of 2.24 eV, this 150°C median life number increases to 81 218 years, and grows to 669 000 years for the switch activation energy of 2.61 eV. Of course, all of these lifetimes increase by about 1000 for operation at 100°C.

Discussion

Although testing was conducted above 220°C for 4380 hours, only two devices degraded beyond the 1 dB failure criterion at the maximum temperature of 260°C. An additional two devices failed because of the mechanical stress required to fixture the devices. These mechanical failures resulted in die cracks which were not considered to be typical of normal device application. Despite the minimal changes that occurred during the test, projections of the degradation was possible, as well as analyses based upon tighter failure criteria. A combination of the projection and tighter failure criteria allowed for predictions of failure distributions, activation energies, and device lifetimes. Each of the four lifetests was found to be lognormally distributed. Correlation to lognormal distributions were found to be generally better than 0.9 with some correlations as high as 0.999. Lognormal sigmas (slopes) were found to be dependent on temperature and to a lesser degree, failure criteria. These effects also created a dependence of activation energy with temperature and failure criteria, as well as, some differences between device types. The activation energy ranged from 1.7 for attenuators to 2.5 for switches, both estimated with a 1 dB failure criterion. Based upon the combination of all the data, lifetimes would be expected to exceed 100 million hours at 150°C (hot spot) operation (Fig. 8). These results compare favorably with previously published results [1], [2].

Conclusions

These tests indicate that high temperature lifetesting is possible utilizing individually forced temperatures while under RF bias. Step stress testing was found to be an important precursor to lifetesting. The precision of a monitored lifetest system heating only the device case has demonstrated that device degradation, failure distributions, and activation energy measurements can be made on small sample sizes with reasonable results. Wearout degradation is caused by gate metal sinking into the channel. Under highly accelerated conditions, these devices have very little drift over time. The degradation that occurred was linear, at least for the duration of this lifetest. Assuming the linear degradation continued, failures would occur in a lognormal manner. The distribution parameters of the projected degradation indicates increasing shape factor (σ) with temperature. Comparison of these results to similar tests under dc bias indicate there is no significant difference between RF biased lifetesting and dc lifetesting for these types of devices. Assuming the least reliable median life at highest stress and the lowest projected activation energy, a conservative estimate of median lifetimes for the switch and attenuator, operating at 150°C peak hot spot temperature and under maximum RF bias, is 18.7 million hours or 2137 years.

References

[1] M. Peters and T. Rubalcava, "Reliability characterization of a production GaAs MMIC amplifier," in *Proc. GaAs REL Workshop*, Nov. 1988, Nashville, TN.

[2] M. Peters, B. Roesch and T. Rubalcava, "Studying lifetimes and failure rates of GaAs MMICs," *Microwaves and RF*, July 1988.

William J. Roesch earned the B.S.E.E. from Oregon State University.

He is presently Manager of the Reliability Engineering Group at TriQuint, with eleven years of experience in semiconductor reliability, evaluation, and failure analysis. In work at Tektronix, between 1971 and 1975, Mr. Roesch was responsible for reliability assurance of various purchased devices. He has performed tests on many IC packages and worked to prove the reliability of plastic encapsulated RAMs and surface mount technology for implementation at Tektronix.

He is currently Chairman of JC-50.1, a JEDEC Committee working on Reliability and Quality of GaAs Devices. Mr. Roesch has published 12 papers on the Reliability of integrated circuits.

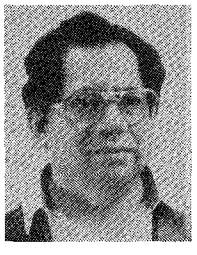

Anthony Rubalcava received a certificate in electronics from West Valley Junior College at Saratoga, CA, and is currently enrolled at Portland Community College pursuing a degree in electronic engineering technology.

He is the Reliability Engineer in charge of microwave devices at TriQuint and has been with the TriQuint Reliability Engineering Group for the past nine years. In earlier work at Tektronix, between 1979 and 1983, Mr. Rubalcava was a Senior Electronic Technician on the manufacturing line of Tektronix' 1-26 GHz 49× Spectrum Analyzer. During this time, he was chosen to join the project team re-designing the 49× phase lock. Before joining Tektronix, from 1974 to 1979, he was an Electronic Technician at Omniyig Inc., where he worked on 1 to 20 GHz YIG tuned oscillators, filters, and multipliers.

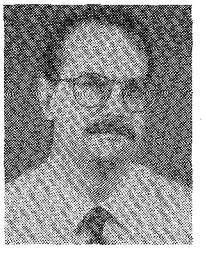

Clark D. Hanson received the B.S. degree in electrical engineering from Colorado State University, Fort Collins, Colorado, in 1975.

In 1975, he joined Motorola's Government Electronics Group in Scottsdale, AZ, where he has been involved in military and commercial reliability programs. For the past four years, he has been extensively involved in GaAs reliability issues with the Strategic Electronics Division of Motorola GEG in Chandler, AZ. He is presently engaged in reliability evaluations of GaAs devices, specifically high power metal-semiconductor field-effect transistor (MESFET) and pseudomorphic high electron mobility transistor (PHEMT) monolithic microwave integrated circuits (MMICs) for use in a commercial satellite constellation which will provide global portable communications.